Synthesis and Characterization of New Triangulo Derivatives of Pt^{I}Pt^{I}Pt^{II}, Including the First Platinum Cluster Binding Both Ethylene and CO

Piero Leoni,*,[†] Fabio Marchetti,[†] Marco Pasquali,[†] Lorella Marchetti,[†] and Alberto Albinati[‡]

Dipartimento di Chimica e Chimica Industriale, Università di Pisa, Via Risorgimento 35, I-56126 Pisa, Italy, and Istituto di Chimica Farmaceutica, Università di Milano, Viale Abruzzi 42, I-20131 Milano, Italy

The terminal hydride in the Pt^{I}Pt^{I}Pt^{II} triangulo cluster Pt$_3$(μ-PBu$^t_2$)$_3$(H)(CO)$_2$ (**1**) may be removed by one-electron oxidants such as [Cp$_2$Fe]PF$_6$. Under carbon monoxide the reaction affords the symmetrical, cationic derivative [Pt$_3$(μ-PBu$^t_2$)$_3$(CO)$_3$]PF$_6$ (**2**). By operating with an excess of the suitable ligand, we also prepared [Pt$_3$(μ-PBu$^t_2$)$_3$(CO)$_2$(NCCH$_3$)]PF$_6$ (**3**) and [Pt$_3$(μ-PBu$^t_2$)$_3$(CO)$_2$(CH$_2$=CH$_2$)]PF$_6$ (**4**). New neutral triangular precursors were obtained by substitution of the CO ligands contained in **1** with isocyanides. The hydrides Pt$_3$(μ-PBu$^t_2$)$_3$-(H)(CNR)$_2$ (**5**, R = CH$_2$Ph; **6**, R = C$_6$H$_4$-p-CH$_3$; **7**, R = Bu^t) were isolated by this route. Complex **7** reacts with chloroform to give Pt$_3$(μ-PBu$^t_2$)$_3$(Cl)(CNBu^t)$_2$ (**8**), which, under an excess of CNBu^t, yields the cationic derivative [Pt$_3$(μ-PBu$^t_2$)$_3$(CNBu^t)$_3$]Cl (**9**). The new triangulo clusters were characterized by multinuclear NMR spectroscopy and, as far as **4** and **7** are concerned, by single-crystal X-ray diffraction.

Introduction

The acidity of metal hydrides can increase by several orders of magnitude when the metal is oxidized, and as a consequence, electron transfer is often followed by deprotonation in the presence of a suitable base.[1,2] Opposite to a simple deprotonation reaction, the aforementioned sequence removes the electrons of the M−H bond, therefore constituting a useful procedure for the generation of a vacant site. This has been shown mainly for piano-stool complexes of Cr, Mo, W,[1] or Ru[2] but may also find application in the chemistry of other metal hydrides[3] or polyhydrides.[4]

We recently found this procedure at work in the reaction of [Cp$_2$Fe]PF$_6$ with the dinuclear platinum(II) dihydride [Pt(μ-PBu$^t_2$)(H)(PBu$^t_2$H)]$_2$, to give a 1:1 mixture of the cations [Pt$_2$(μ-PBu$^t_2$)$_2$(H)(PBu$^t_2$H)$_2$]PF$_6$ and [Pt$_2$(μ-PBu$^t_2$)(μ-H)(PBu$^t_2$H)$_3$(H)]PF$_6$, the former being quantitatively formed in the presence of NEt$_3$.[5]

Some related aspects of the reactivity of [Pt$_3$(μ-PBu$^t_2$)$_3$(CO)$_2$(H)] (**1**)[6] will be outlined in the following discussion. Oxidant-induced ([Cp$_2$Fe]PF$_6$) deprotonation of complex **1** creates a vacant site suitable for coordination of other molecules; in the presence of CO, MeCN, or ethylene the reaction ends up, respectively, with the formation of [Pt$_3$(μ-PBu$^t_2$)$_3$(CO)$_3$]PF$_6$ (**2**), [Pt$_3$(μ-PBu$^t_2$)$_3$-(CO)$_2$(NCMe)]PF$_6$ (**3**), or [Pt$_3$(μ-PBu$^t_2$)$_3$(CO)$_2$(CH$_2$=CH$_2$)]-PF$_6$ (**4**). Moreover, new hydride precursors were prepared by reacting complex **1** with isocyanides. The X-ray crystal and molecular structure of **4**, an unprecedented example of a platinum cluster bearing both ethylene and CO ligands, and of Pt$_3$(μ-PBu$^t_2$)$_3$(H)(CNBu^t)$_2$ (**7**) are also reported.

Results and Discussion

Preparation of [Pt$_3$(μ-PBu$^t_2$)$_3$(CO)$_2$(L)]PF$_6$ (L = CO, CH$_3$CN, CH$_2$=CH$_2$). A strong excess of Na$_2$CO$_3$ and 2 equiv of [Cp$_2$Fe]PF$_6$ were added to a CO-saturated DME solution of complex **1**. After workup a red solid was isolated and identified as [Pt$_3$(μ-PBu$^t_2$)$_3$(CO)$_3$]PF$_6$ (**2**) (eq 1).

All NMR spectra consist of the usual sum of subspectra arising from the various isotopomers with different contents of the NMR-active ^{195}Pt nucleus ($I = {}^1/_2$, NA = 33.8%); the numbering scheme and a table showing the isotopomer's composition and relative abundance is shown in Table 1.

As expected, the ^{31}P{^{1}H} NMR spectrum of cation **2**$^+$ exhibits only a low-field singlet (154.6 ppm, isotopomer **A**, Figure 1).[7] In the ^{195}Pt-containing isotopomers **B**−**H** the P nuclei (as well as the Pt nuclei in **E**−**H**) lose their magnetic equivalence and the satellites appear quite complex and cannot be interpreted in a simple first-

† Università di Pisa.
‡ Università di Milano.
(1) (a) Ryan, O. B.; Tilset, M.; Parker, V. *J. Am. Chem. Soc.* **1990**, *112*, 2618. (b) Smith, K. T.; Tilset, M. *J. Organomet. Chem.* **1992**, *431*, 55. (c) Quadrelli, E, A.; Kraatz, H.-B.; Poli, R. *Inorg. Chem.* **1996**, *35*, 5154.
(2) (a) Ryan, O. B.; Tilset, M. *J. Am. Chem. Soc.* **1991**, *113*, 9554. (b) Ryan, O. B.; Tilset, M.; Parker, V. D. *Organometallics* **1991**, *10*, 298.
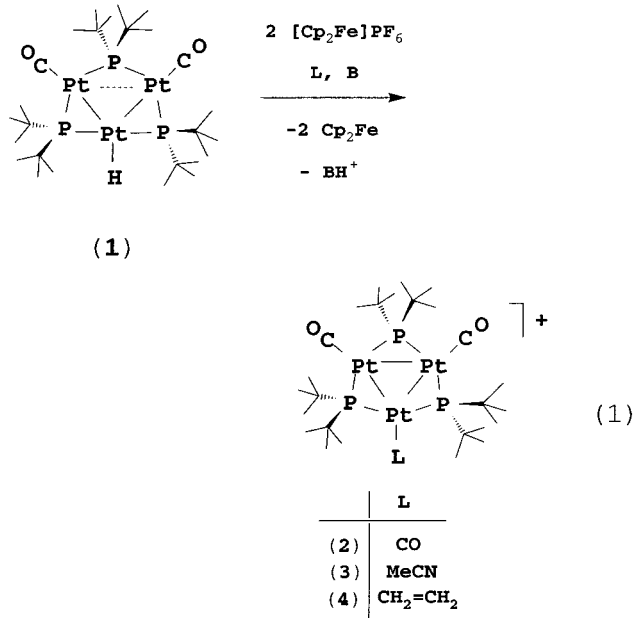(3) Marken, F.; Bond, A. M.; Colton, R. *Inorg. Chem.* **1995**, *34*, 1705.
(4) (a) Detty, M. R.; Jones, W. D. *J. Am. Chem. Soc.* **1987**, *109*, 5666. (b) Zlota, A. A.; Tilset, M.; Caulton, K. G. *Inorg. Chem.* **1993**, *32*, 3816.
(5) Leoni, P.; Pasquali, M.; Fortunelli, A.; Germano, G.; Albinati, A. *J. Am. Chem. Soc.*, **1998**, *120*, 9564.
(6) Leoni, P.; Manetti, S.; Pasquali, M.; Albinati, A. *Inorg. Chem.* **1996**, *35*, 6045.

(7) The expected septet ($^1J_{PF}$ = 708 Hz) due to the PF$_6^-$ anion was also observed at −139 ppm.

order approximation; the same holds for the unique ^{195}Pt{^{1}H} NMR signal at −5950 ppm (Figure 2). Both spectra were satisfactorily simulated by the following coupling constants: $^2J_{PP}$ = 130, $^1J_{PPt}$ = 1786, $^2J_{PPt}$ = −100, $^1J_{PtPt}$ = 1800 Hz.

The ^{1}H NMR spectrum (1.37 ppm, virtual triplet, $^3J_{HP}$ + $^5J_{HP}$ = 7 Hz, Bu^t), strong ν$_{CO}$ absorptions (2095 and 2033 cm^{-1} (Nujol), 2064 cm^{-1} (CHCl$_3$)) in the IR spectrum, and the elemental analyses agree well with the proposed structure; the same cation has recently been isolated as the triflate salt through a different synthetic procedure, and an X-ray study[8] has confirmed the structure shown in eq 1.

The oxidation of **1**, carried out in acetonitrile, gives complex mixtures of products in the absence of a base or with added Et$_3$N or Na$_2$CO$_3$. In the presence of lutidine, previously employed in the oxidation of Ru hydrides,[2b,4b] we isolated in good yields [Pt$_3$(μ-PBu$^t_2$)$_3$-(NCCH$_3$)(CO)$_2$]PF$_6$ (**3**) as a deep green solid. The ^{31}P{^{1}H} NMR spectrum (CDCl$_3$, 293 K) of **3** shows the expected two signals at 152.5 (t, P$_3$) and 95.7 (d, P$_{1,2}$) ppm ($^2J_{PP}$ = 132 Hz), the latter being significantly high-field shifted by the adjacent σ-donor CH$_3$CN ligand (for analogous shifts see the spectra of **1** and of complexes **5**−**9** below). Both signals are flanked by ^{195}Pt satellites reproduced in a simulation by using the coupling constants given in Table 1. The same values were used to reproduce the shape of the ^{195}Pt{^{1}H} NMR (CD$_3$CN, 293 K) signals at −5533.6 (Pt$_{1,3}$) and −6503 (broad, Pt$_2$) ppm. Significant signals were observed at 2024 and 2000 cm^{-1} (ν$_{CO}$, Nujol) and at 2.81 ppm (s, CH_3CN), respectively, in the IR and ^{1}H NMR (CDCl$_3$, 293 K) spectra.

When complex **1** was reacted with 2 equiv of [Cp$_2$Fe]-PF$_6$ and a strong excess of Na$_2$CO$_3$ under 1 atm of ethylene, the new complex [Pt$_3$(μ-PBu$^t_2$)$_3$(CH$_2$=CH$_2$)-(CO)$_2$]PF$_6$ (**4**) was isolated in moderate yields (46%) as a red microcrystalline solid. Single crystals for the X-ray study (see below) were obtained by recrystallization

(8) Leoni, P.; Marchetti, F.; Mealli, C.; Pasquali, M.; Quaglierini, S. Manuscript in preparation.

from CH$_2$Cl$_2$/Et$_2$O mixtures. Complex **4** exhibits ν$_{CO}$ absorptions at 2049 and 2035 cm^{-1} (Nujol) in the IR spectrum and, in the ^{1}H NMR spectrum (CDCl$_3$, 293 K), a slightly broadened singlet at 4.42 ppm with ^{195}Pt satellites ($^2J_{HPt}$ = 68 Hz). These values compare well with those found in the known platinum ethylene derivatives.[9] The signals due to atoms P$_{1,2}$ and P$_3$ are nearly overlapped at ca. 168 ppm in the ^{31}P{^{1}H} NMR spectrum, therefore resulting in a very complex higher order pattern. This and the ^{195}Pt{^{1}H} NMR spectrum (signals at −6142 (Pt$_{1,3}$) and −6358 (Pt$_2$) ppm, Figure 3a,b) were satisfactorily reproduced by a simulation employing the parameters shown in Table 1. As expected, the signal at −6358 ppm splits for the coupling to the four ethylene protons in the proton-coupled ^{195}Pt NMR spectrum (Figure 3c).

The overall reactions of **1** shown above can be seen as the formal oxidation of the hydride ligand to H$^+$, which is removed by the added base, and the addition of a new neutral ligand to the unsaturated [Pt$_3$(μ-PBu$^t_2$)$_3$(CO)$_2$]$^+$ cation. Therefore, the final products **2**−**4** share both the valence electron count (44 e$^-$) and the platinum oxidation numbers (Pt^{I}Pt^{I}Pt^{II}) with their precursor **1**. It is worth noting that a Pt^{I}Pt^{I}Pt^{II} cation, namely [Pt$_3$(μ-PBu$^t_2$)$_2$(μ-H)(PBu$^t_2$H)(CO)$_2$]$^+$, was also formed when **1** was reacted with triflic acid.[10a] In that case the oxidation caused by protonation was counterbalanced by the reductive P−H coupling of the hydride with an adjacent phosphide; a very similar reaction, yielding [Pt$_3$(μ-PPh$_2$)$_2$(μ-I)(PPh$_3$)$_3$]I after P−C reductive coupling, occurs between I$_2$ and Pt$_3$(μ-PPh$_2$)$_3$(Ph)-(PPh$_3$)$_2$, a triangular platinum complex strictly related to **1**.[10b]

Preparation of Pt$_3$(μ-PBu$^t_2$)$_3$(CNR)$_2$(H) (R = CH$_2$Ph, C$_6$H$_4$-*p*-CH$_3$, Bu^t). Other hydride precursors can be prepared through the substitution of the carbonyl ligands in **1** with alkyl or aryl isocyanides (RNC; R = CH$_2$Ph, C$_6$H$_4$-*p*-CH$_3$, Bu^t). The reactions with 2 equiv of RNC quickly and cleanly afford the corresponding disubstituted derivatives Pt$_3$(μ-PBu$^t_2$)$_3$(CNR)$_2$(H) (**5**, R = CH$_2$Ph; **6**, R = C$_6$H$_4$-*p*-CH$_3$; **7**, R = Bu^t) as red-brown microcystalline solids. Complexes **5**−**7** were characterized by elemental and spectroscopic analyses; single crystals of **7** (see below) were grown by recrystallization from *n*-hexane. The NMR spectra are very similar to the corresponding spectra discussed in detail for complex **1**,[6] and their analyses gave the parameters shown in Table 1.
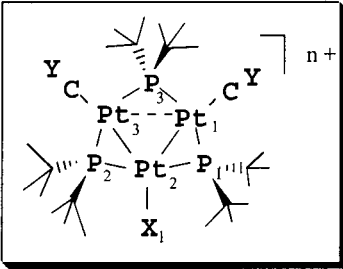
The trinuclear hydrides **5**−**7** slowly decompose in chloroform. In the case of complex **7** the decomposition was deliberately followed until complete conversion (60 °C, 12 h) into the corresponding chloride Pt$_3$(μ-PBu$^t_2$)$_3$-(CNBu^t)$_2$(Cl) (**8**), which was isolated in 62% yield. As expected, the NMR spectra of **8** (Table 1) are similar to those of its precursor, except for the lack of the hydride

(9) (a) Ikura, K.; Ryu, I.; Ogawa, A.; Sonoda, N.; Harada, S.; Kasai, N. *Organometallics* **1991**, *10*, 528. (b) Basickes, N.; Hutson, A. C.; Sen, A.; Yap, G. P. A.; Rheingold, A. L. *Organometallics* **1996**, *15*, 4116. (c) Delis, J. G. P.; van Leeuwen, P. W. N. M.; Vrieze, K.; Veldman, N.; Spek, A. J.; Fraanje, J.; Goubitz, K. *J. Organomet. Chem.* **1996**, *514*, 125. (d) Albinati, A.; Isaia, F.; Kaufmann, W.; Sorato, C.; Venanzi, L. M. *Inorg. Chem.* **1989**, *28*, 1112. (e) Scott, J. D.; Puddephatt, R. J. *Organomtallics* **1986**, *5*, 1253.
(10) (a) Fortunelli, A.; Leoni, P.; Marchetti, L.; Pasquali, M.; Sbrana, F.; Selmi, M. *Inorg. Chem.* **2001**, *40*, 3055. (b) Archambault, C.; Bender, R.; Braunstein, P.; De Cian, A.; Fisher, J. *Chem. Commun.* **1996**, 2729.

Table 1. Selected NMR Parameters (δ in ppm and J in Hz) for Complexes 1–9

Isotop	Pt$_1$	Pt$_2$	Pt$_3$	%
A	-	-	-	29.0
B	^{195}Pt	-	-	14.8
C	-	^{195}Pt	-	14.8
D	-	-	^{195}Pt	14.8
E	^{195}Pt	^{195}Pt	-	7.6
F	^{195}Pt	-	^{195}Pt	7.6
G	-	^{195}Pt	^{195}Pt	7.6
H	^{195}Pt	^{195}Pt	^{195}Pt	4.8

Compl	X	Y	n
1	H	O	0
2	CO	O	1
3	MeCN	O	1
4	CH$_2$CH$_2$	O	1
5	H	NCH$_2$Ph	0
6	H	N-○	0
7	H	NBu^t	0
8	Cl	NBu^t	0
9	CNBu^t	NBu^t	1

	1	2	3	4	5	6	7	8	9
$\delta_{P_{1,2}}$	216.9	154.6	152.5	168.1	196.1	197.8	173.0	131.8	139.5
δ_{P_3}	95.2	154.6	95.7	166.6	101.4	97.8	99.0	71.7	139.5
$\delta_{Pt_{1,3}}$	−5611	−5950	−5534	−6143	−5792	−5715	−5925	−5636	−6111
δ_{Pt_2}	−6893	−5950	−6503	−6375	−6909	−6895	−6827	−6476	−6111
δ_{H_1}	−6.58				−5.70	−5.53	−4.30		
$^2J_{P_1P_3}$, $^2J_{P_2P_3}$	152	130	132	124	171	167	167	160	165
$^2J_{P_1P_2}$	164	130	220	142	198	194	229	155	165
$^1J_{P_1P_3}$, $^1J_{Pt_3P_3}$	2064	1786	1690	1808	2131	2117	2112	1869	1990
$^1J_{Pt_1P_1}$, $^1J_{Pt_3P_2}$	2541	1786	1893	1820	2400	2370	2200	1973	1990
$^1J_{Pt_2P_1}$, $^1J_{Pt_2P_2}$	2022	1786	2220	1890	2198	2188	2275	2387	1990
$^2J_{Pt_2P_3}$	−253	−100	−122	−117	−181	−191	−120	−136	−102
$^2J_{Pt_1P_2}$, $^2J_{Pt_3P_1}$	−116	−100	−88	−116	−16	−50	−45	−118	−102
$^1J_{Pt_1Pt_3}$	650	1800	1700	1700	650	650	550	a	1550
$^1J_{Pt_1Pt_2}$, $^1J_{Pt_3Pt_2}$	780	1800	2356	1948	780	705	750	2180	1550
$^1J_{Pt_2H_1}$	1250				1367	1360	1536		
$^2J_{Pt_1H_1}$, $^2J_{Pt_3H_1}$	59				41	60	a		
$^2J_{P_1H_1}$, $^2J_{P_2H_1}$	8.4				9	9	8		
$^3J_{P_3H_1}$	18				11	10	a		

^{a} Not detected due to line broadening.
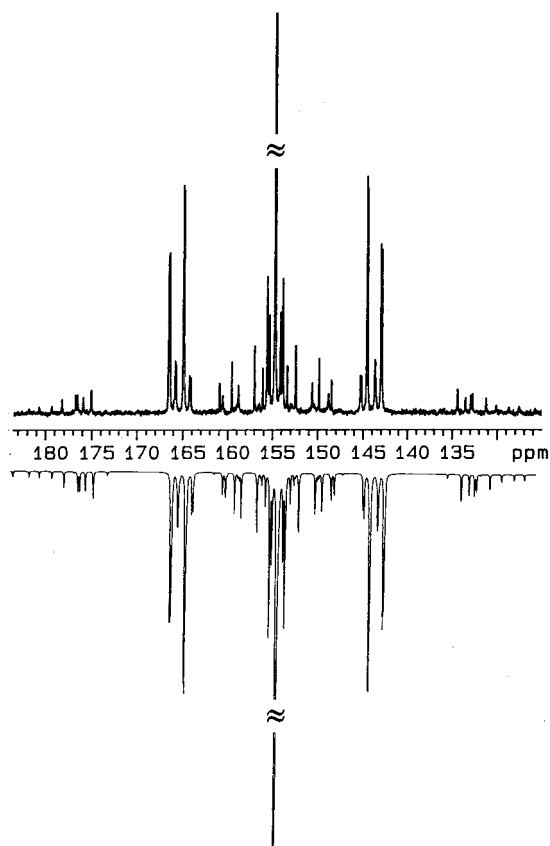
Figure 1. Experimental (top) and calculated (bottom) ^{31}P{^{1}H} NMR spectra (CDCl$_3$, 293 K) of complex **2**.
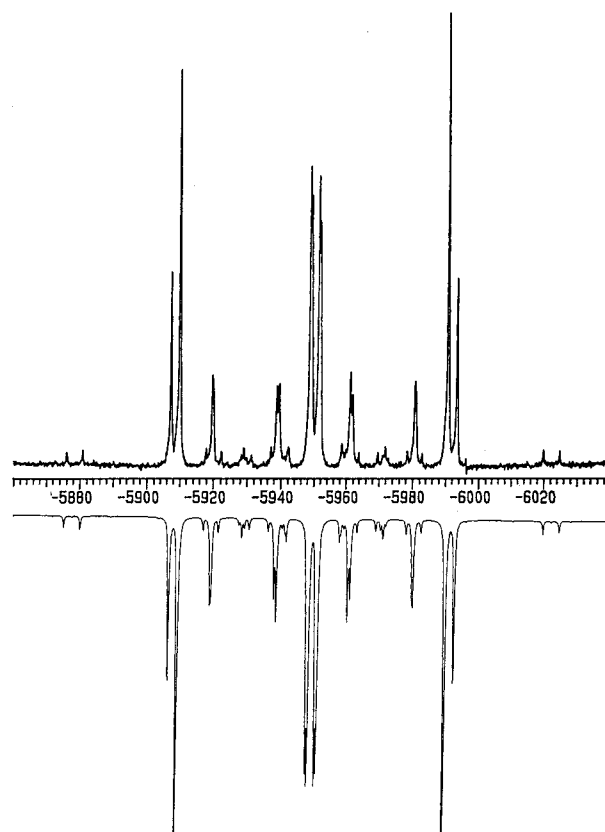
Figure 2. Experimental (top) and calculated (bottom) ^{196}Pt{^{1}H} NMR spectra (CDCl$_3$, 293 K) of complex **2**.

signal in the ^{1}H NMR spectrum. In the presence of an excess of Bu^{t}NC, complex **8** is transformed into the

symmetrical cationic derivative [Pt$_3$(μ-PBu$^t_2$)$_3$(CNBu^t)$_3$]-Cl (**9**). In contrast to complex **8**, **9** is easily soluble in
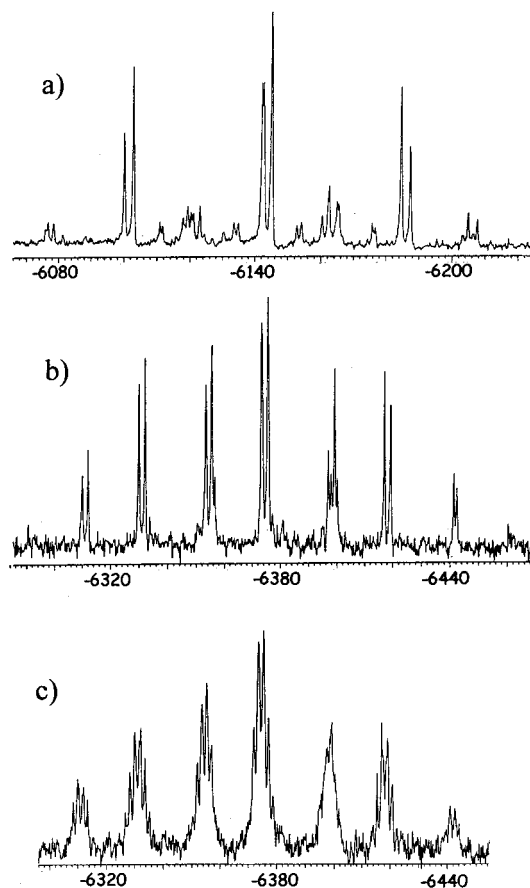
Figure 3. ^{196}Pt NMR (CDCl$_3$, 293 K) signals observed for complex **4**: (a) Pt$_{1,3}$, proton decoupled; (b) Pt$_2$, proton decoupled; (c) Pt$_2$, proton coupled.
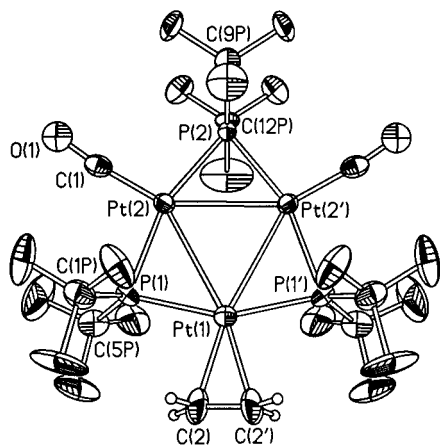

Figure 4. Molecular structure of the cation [Pt$_3$(μ-PBu$^t_2$)$_3$-(CO)$_2$(C$_2$H$_4$)]$^+$. Thermal ellipsoids are drawn at the 30% probability level. Primed atoms are defined as in Table 2.

polar solvents and insoluble in apolar solvents; its ^{31}P and ^{195}Pt NMR spectra (δ_p 139.4 (s, with satellites), δ_{Pt} −6111 (dt) ppm, $^1J_{PtP}$ = 1990, $^2J_{PtP}$ = 119 Hz) show features similar to the corresponding spectra of the symmetrical tricarbonyl **2**.

Crystal Structure of [Pt$_3$(μ-PBu$^t_2$)$_3$(CH$_2$=CH$_2$)-(CO)$_2$]PF$_6$ (4). A perspective view of the molecular structure of cation **4**$^+$ is shown in Figure 4, while relevant bond distances and angles are listed in Table 2. The cation has a C_2 symmetry, due to the presence of a 2-fold axis, passing through atom Pt(1) and the

Table 2. Main Bond Lengths (Å) and Angles (deg) for [Pt$_3$(μ-PBu$^t_2$)$_3$(CO)$_2$(C$_2$H$_4$)]$^+$ (4$^+$)^a

Pt(1)−C(2)	2.14(4)	Pt(2)−P(1)	2.316(6)
Pt(1)−C(2′)	2.14(4)	Pt(2)−Pt(2′)	2.913(2)
Pt(1)−P(1)	2.303(6)	C(1)−O(1)	1.21(3)
Pt(1)−P(1′)	2.303(6)	C(2)−C(2′)	1.25(6)
Pt(1)−Pt(2)	3.028(2)	P(1)−C(5P)	1.86(3)
Pt(1)−Pt(2′)	3.028(2)	P(1)−C(1P)	1.88(3)
Pt(2)−C(1)	1.80(3)	P(2)−C(12P)	1.86(3)
Pt(2)−P(2)	2.312(7)	P(2)−C(9P)	1.93(4)
C(2)−Pt(1)−C(2′)	33.8(17)	P(2)−Pt(2)−Pt(1)	112.15(14)
C(2)−Pt(1)−P(1)	85.1(9)	P(1)−Pt(2)−Pt(1)	48.86(16)
C(2)−Pt(1)−P(1′)	118.9(9)	Pt(2′)−Pt(2)−Pt(1)	61.25(2)
P(1)−Pt(1)−P(1′)	156.0(3)	O(1)−C(1)−Pt(2)	174(2)
C(2)−Pt(1)−Pt(2)	134.3(8)	C(2′)−C(2)−Pt(1)	73.1(8)
C(2′)−Pt(1)−Pt(2)	168.2(8)	C(5P)−P(1)−C(1P)	117.0(14)
P(1)−Pt(1)−Pt(2)	49.2(2)	C(5P)−P(1)−Pt(1)	116.2(11)
P(1′)−Pt(1)−Pt(2)	106.7(2)	C(1P)−P(1)−Pt(1)	116.3(10)
C(2)−Pt(1)−Pt(2′)	168.2(8)	C(5P)−P(1)−Pt(2)	109.5(10)
Pt(2)−Pt(1)−Pt(2′)	57.51(4)	C(1P)−P(1)−Pt(2)	110.0(10)
C(1)−Pt(2)−P(2)	99.7(8)	Pt(1)−P(1)−Pt(2)	81.9(2)
C(1)−Pt(2)−P(1)	99.4(8)	C(12P)−P(2)−C(9P)	116.5(16)
P(2)−Pt(2)−P(1)	160.9(2)	C(12P)−P(2)−Pt(2′)	113.2(8)
C(1)−Pt(2)−Pt(2′)	150.4(8)	C(9P)−P(2)−Pt(2′)	115.1(8)
P(2)−Pt(2)−Pt(2′)	50.95(14)	C(12P)−P(2)−Pt(2)	113.2(8)
P(1)−Pt(2)−Pt(2′)	110.10(16)	C(9P)−P(2)−Pt(2)	115.1(8)
C(1)−Pt(2)−Pt(1)	148.2(8)	Pt(2′)−P(2)−Pt(2)	78.1(3)

^{a} Symmetry transformations used to generate equivalent atoms: Primed atoms: x, $-y + \frac{1}{2}$, z.

midpoint of the Pt(2)−Pt(2′) vector; thus only half of **4**$^+$ is independent. The Pt atoms are arranged in an almost equilateral triangle, with rather long Pt−Pt bond distances (Pt(1)−Pt(2),Pt(2′) = 3.028 Å, Pt(2)−Pt(2′) = 2.913 Å (see Table 2)). These distances are longer than those observed in platinum metal (2.774 Å),[11] although still in the range reported for metal−metal-bonded triangular platinum frameworks.[12−14]

The Pt−Pt bonds are bridged by phosphido ligands (Pt(1)−P(1)−Pt(2) = 81.9°, Pt(2)−P(2)−Pt(2′) = 78.1°), with the P atoms lying approximately on the plane defined by the platinum atoms (maximum deviation 0.089(8) Å). The carbon atoms of the carbonyl and ethylene ligands also lie in this plane (maximum deviation 0.063 Å). The C−C bond distance is 1.28(6) Å (1.344 Å for ethylene in the gas phase); the large esd is probably due to significant oscillations of the ligand around its centroid.

Crystal Structure of Pt$_3$(μ-PBu$^t_2$)$_3$(H)(CNBu^t)$_2$ (7). An ORTEP view of compound **7** is shown in Figure 5, while a selection of bond lengths and angles is listed in Table 3.

The "Pt$_3$(μ-P)$_3$" moiety may approximately be described as an "equilateral triangle" with Pt−Pt separa-

(11) Teatum, E. T.; Gschneider, K. Jr.; Waber, J. T. 1968 Compilation of Calculated Data Useful in Predicting Metallurgical Behavior of the Elements in Binary Alloy Systems; USAEC Report LA-4003, 1968 (supersedes Report LA-2345, 1960).
(12) (a) Bott, S. G.; Hallam, M. F.; Ezomo, O. J.; Mingos, D. M. P.; Williams, I. D. *J. Chem. Soc., Dalton Trans.* **1988**, 1461. (b) Evans, D. G.; Hughes, G. R.; Mingos, D. M. P.; Basset, J.-M.; Welch, A. J. *J. Chem. Soc., Dalton Trans.* **1988**, 1509. (c) Bellon, P. L.; Longoni, G. *J. Chem. Soc., Chem. Commun.* **1980**, 1255. (d) Scherer, O. J.; Konrad, R.; Guggolz, E.; Ziegler, M. L. *Chem. Ber.* **1985**, *118*, 1. (e) Green, M.; Howard, J. A.; Murray, M.; Spencer, J. M.; Stone, F. G. A. *J. Chem. Soc., Dalton Trans.* **1977**, 1509. (f) Ferguson, G.; Lloyd, B. R.; Puddephatt, R. J. *Organometallics* **1986**, *5*, 344.
(13) (a) Bender, R.; Braunstein, P.; Dedieu, A.; Ellis, P. D.; Huggins, B.; Harvey, P. D.; Sappa, E.; Tiripicchio, A. *Inorg. Chem.* **1996**, *35*, 1223. (b) Bender, R.; Braunstein, P.; Tiripicchio. A.; Tiripicchio Camellini, M. *Angew. Chem., Int. Ed. Engl.* **1985**, *24*, 861.
(14) Taylor, N. J.; Chieh, P. C.; Carty, A. J. *J. Chem. Soc., Chem. Commun.* **1975**, 448.
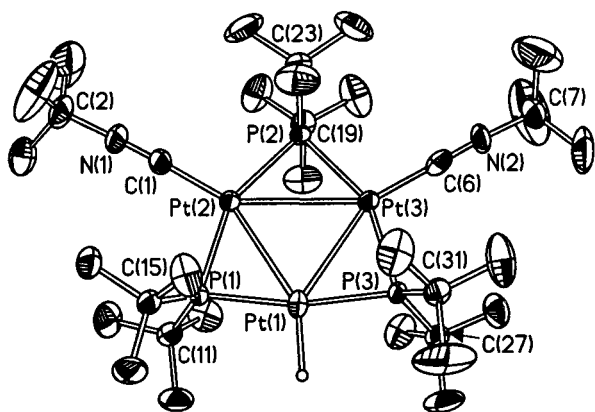
Figure 5. Molecular structure of $[Pt_3(\mu\text{-}PBu^t_2)_3(CN^tBu)_2\text{-}(H)]$. Thermal ellipsoids are drawn at the 50% probability level.

Table 3. Bond Lengths (Å) and Angles (deg) for $[Pt_3(\mu\text{-}PBu^t_2)_3(CN^tBu)_2(H)]\cdot 0.5C_6H_{14}$ ($7\cdot 0.5C_6H_{14}$)

Pt(1)–P(3)	2.244(2)	P(1)–C(11)	1.870(11)
Pt(1)–P(1)	2.247(2)	P(1)–C(15)	1.887(10)
Pt(1)–Pt(3)	2.9014(8)	P(2)–C(19)	1.882(9)
Pt(1)–Pt(2)	2.9145(7)	P(2)–C(23)	1.886(11)
Pt(2)–C(1)	1.892(11)	P(3)–C(27)	1.869(9)
Pt(2)–P(1)	2.289(2)	P(3)–C(31)	1.870(10)
Pt(2)–P(2)	2.293(2)	C(1)–N(1)	1.152(12)
Pt(2)–Pt(3)	3.1709(8)	N(1)–C(2)	1.430(14)
Pt(3)–C(6)	1.898(12)	C(6)–N(2)	1.155(13)
Pt(3)–P(3)	2.289(2)	N(2)–C(7)	1.419(14)
Pt(3)–P(2)	2.290(2)		

P(3)–Pt(1)–P(1)	167.53(8)	P(2)–Pt(3)–Pt(2)	46.25(6)
P(3)–Pt(1)–Pt(3)	50.90(5)	Pt(1)–Pt(3)–Pt(2)	57.16(2)
P(1)–Pt(1)–Pt(3)	116.70(6)	C(11)–P(1)–C(15)	113.0(5)
P(3)–Pt(1)–Pt(2)	116.90(6)	C(11)–P(1)–Pt(1)	116.0(3)
P(1)–Pt(1)–Pt(2)	50.65(6)	C(15)–P(1)–Pt(1)	115.0(3)
Pt(3)–Pt(1)–Pt(2)	66.08(2)	C(11)–P(1)–Pt(2)	113.7(3)
C(1)–Pt(2)–P(1)	103.4(3)	C(15)–P(1)–Pt(2)	115.4(3)
C(1)–Pt(2)–P(2)	104.4(3)	Pt(1)–P(1)–Pt(2)	79.95(7)
P(1)–Pt(2)–P(2)	152.12(8)	C(19)–P(2)–C(23)	113.3(5)
C(1)–Pt(2)–Pt(1)	152.6(3)	C(19)–P(2)–Pt(3)	113.0(3)
P(1)–Pt(2)–Pt(1)	49.40(6)	C(23)–P(2)–Pt(3)	113.8(4)
P(2)–Pt(2)–Pt(1)	102.91(6)	C(19)–P(2)–Pt(2)	113.2(4)
C(1)–Pt(2)–Pt(3)	150.4(3)	C(23)–P(2)–Pt(2)	113.6(3)
P(1)–Pt(2)–Pt(3)	106.14(6)	Pt(3)–P(2)–Pt(2)	87.57(7)
P(2)–Pt(2)–Pt(3)	46.17(5)	C(27)–P(3)–C(31)	112.7(4)
Pt(1)–Pt(2)–Pt(3)	56.76(2)	C(27)–P(3)–Pt(1)	116.2(3)
C(6)–Pt(3)–P(3)	103.7(3)	C(31)–P(3)–Pt(1)	116.0(3)
C(6)–Pt(3)–P(2)	103.5(3)	C(27)–P(3)–Pt(3)	115.1(3)
P(3)–Pt(3)–P(2)	152.87(8)	C(31)–P(3)–Pt(3)	113.4(3)
C(6)–Pt(3)–Pt(1)	153.0(3)	Pt(1)–P(3)–Pt(3)	79.58(7)
P(3)–Pt(3)–Pt(1)	49.52(5)	N(1)–C(1)–Pt(2)	176.4(10)
P(2)–Pt(3)–Pt(1)	103.38(6)	C(1)–N(1)–C(2)	174.5(13)
C(6)–Pt(3)–Pt(2)	149.7(3)	N(2)–C(6)–Pt(3)	178.2(9)
P(3)–Pt(3)–Pt(2)	106.62(5)	C(6)–N(2)–C(7)	176.1(12)

tions at 2.9624(3), 2.9485(3), and 3.0906(3) Å, respectively. This geometry is comparable with that found in $Pt_3(\mu\text{-}PPh_2)_3(Ph)(PPh_3)_2$ (**10**).[13,14] where the metal–metal distances are 2.956(3) and 3.073(4) Å respectively. We note that **10** was the first reported example of a compound showing a reversible skeletal isomerism; by changing the crystallization solvent, a second isomeric form, with different metal separations in the "$Pt_3(\mu\text{-}P)_3$" group, can be isolated. In the latter isomer, the Pt–Pt distances are 2.785(3) and 3.586(2) Å, respectively, showing the existence of a very soft potential for the deformation of the "$Pt_3(\mu\text{-}P)_3$" core; the switching between the two geometries may be due to the packing forces. It may be also interesting to note the following.

(1) Compound **1**, the precursor of **7**, always crystallizes in the latter geometry (Pt–Pt distances being 2.716, 2.725, and 3.614 Å, respectively).

(2) The substitution of the CO ligands in **1**, with the isocyanides in compound **7**, always yields the "equilateral triangle" geometry; this is in agreement with the results of a theoretical modeling of two isomers of **10**. It has been shown[13] that small energy differences between the two forms may be expected in asymmetrically substituted 44 e$^-$ clusters such as $Pt_3(\mu\text{-}PR_2)_3(L)_2$-(X) and that the more easily elongated metal–metal bond is the one opposite to the σ-donor ligand. Moreover, further evidence of the softness of the deformation potential may be found by comparing the values of the Pt–Pt separations (see Table 3) at 200 K with those at room temperature: 2.9145(7), 2.9014(8), and 3.1709 Å, respectively (see the Supporting Information).

All other distances in **7** are unexceptional and do not show significant changes as a function of the temperature.

The bridging phosphido ligands deviate slightly from the plane defined by the Pt atoms (P1, -0.06 Å; P2, -0.08 Å; P3, $+0.11$ Å), while larger deviations are observed for the CN groups (in the range ± 0.1–0.2 Å).

Experimental Section

General Data. The reactions were carried out under a nitrogen atmosphere, by using standard Schlenk techniques. $Pt_3(\mu\text{-}PBu^t_2)_3(H)(CO)_2$ (**1**) was prepared as previously described.[6] Solvents were dried by conventional methods and distilled under nitrogen prior to use. IR spectra (Nujol mulls, KBr) were recorded on a Perkin-Elmer FT-IR 1725X spectrophotometer. NMR spectra were recorded on a Varian Gemini 200 BB instrument; frequencies are referenced to the residual resonances of the deuterated solvent (H, ^{13}C), 85% H_3PO_4 (^{31}P), and H_2PtCl_6 (^{195}Pt).

Preparation of $[Pt_3(\mu\text{-}PBu^t_2)_3(CO)_3]PF_6$ (2). $[Cp_2Fe]PF_6$ (75 mg, 0.226 mmol) and Na_2CO_3 (122 mg, 1.15 mmol) were added to a solution of complex **1** (122 mg, 0.113 mmol) in DME (6 mL). The flask was evacuated and filled with CO (1 atm), and the suspension was stirred for 3 h at room temperature. The suspension was filtered, and the red solid formed in the reaction was extracted with dichloromethane. Unreacted insoluble reagents were filtered off, and the red solution was concentrated to ca. 2 mL. After the addition of Et$_2$O (10 mL) a red solid precipitated out and was separated by filtration, washed with Et$_2$O, and vacuum-dried (52 mg, 52% yield).

Anal. Calcd for $C_{27}H_{54}F_6O_3P_4Pt_3$: C, 26.0; H, 4.35. Found: C, 26.4; H, 4.91. ^{1}H NMR (acetone-d_6, 293 K): δ 1.37 (vt, $^3J_{HP} + {}^5J_{HP} = 7$ Hz, 54 H, PCCH_3) ppm. ^{13}C{^{1}H} NMR (acetone-d_6, 293 K): δ 47.5 (s, PC), 31.3 (s, PCCH_3) ppm. IR (Nujol, KBr): 2095, 2033 (ν_{CO}). IR (CHCl$_3$): 2064 (ν_{CO}) cm^{-1}.

Preparation of $[Pt_3(\mu\text{-}PBu^t_2)_3(CO)_2(NCCH_3)]PF_6$ (3). $[Cp_2Fe]PF_6$ (88 mg, 0.266 mmol) and lutidine (24 μL, 0.206 mmol) were added to a solution of complex **1** (142 mg, 0.132 mmol) in CH$_3$CN (7 mL). After it stood a few minutes at room temperature, the solution was concentrated to ca. 2 mL. When Et$_2$O (10 mL) was added, a deep green solid precipitated out and was separated by filtration, washed with Et$_2$O, and vacuum-dried (125 mg, 75% yield).

Anal. Calcd for $C_{28}H_{57}F_6NO_2P_4Pt_3$: C, 26.6; H, 4.55; N, 1.11 Found: C, 26.5; H, 4.81, N, 1.32. ^{1}H NMR (CDCl$_3$, 293 K): δ 2.81 (s, with satellites, $^4J_{HPt} = 8.4$ Hz, 3 H, NC-CH_3), 1.47 (m, 54 H, Bu^t) ppm. IR (Nujol, KBr): 2024, 2000 (ν_{CO}) cm^{-1}.

Preparation of $[Pt_3(\mu\text{-}PBu^t_2)_3(CO)_2(CH_2=CH_2)]PF$, (4). $[Cp_2Fe]PF_6$ (95 mg, 0.287 mmol) and Na_2CO_3 (138 mg, 1.30 mmol) were added to a solution of complex **1** (140 mg, 0.130 mmol) in DME (7 mL). The flask was evacuated and filled with

ethylene (1 atm). The suspension was stirred for 3 h at room temperature. The suspension was filtered, and the red solid formed in the reaction was extracted with dichloromethane. Unreacted insoluble reagents were filtered off, and the red solution was concentrated to ca. 2 mL. After the addition of Et$_2$O (10 mL) a red solid precipitated out and was separated by filtration, washed with Et$_2$O, and vacuum-dried (72 mg, 46% yield).

Anal. Calcd for C$_{28}$H$_{58}$F$_6$O$_2$P$_4$Pt$_3$: C, 26.9; H, 4.68. Found: C, 27.4; H, 4.60. ^{1}H NMR (CDCl$_3$, 293 K): δ 4.42 (s, with satellites, $^2J_{HPt}$ = 68 Hz, 4 H, =CH_2), 1.51 (d, $^3J_{HP}$ = 16 Hz, 18 H, Bu^t), 1.43 (d, $^3J_{HP}$ = 15 Hz, 36 H, Bu^t) ppm. IR (Nujol, KBr): 2046, 2027 (ν_{CO}) cm^{-1}.

Preparation of Pt$_3$(μ-PBu$^t_2$)$_3$(H)(CNCH$_2$Ph)$_2$ (5). A toluene solution containing 0.335 mmol of PhCH$_2$NC was added to an orange solution of complex **1** (180 mg, 0.167 mmol) in toluene (6 mL). The solution quickly turned brown, and the solvent was evaporated; the residue was suspended in *n*-hexane (6 mL) and left overnight at −30 °C. The brown solid was separated by filtration and vacuum-dried (147 mg, 70% yield).

Anal. Calcd for C$_{40}$H$_{69}$N$_2$P$_3$Pt$_3$: C, 38.2; H, 5.50; N, 2.23. Found: C, 38.4; H, 5.61; N, 2.28. ^{1}H NMR (CDCl$_3$, 293 K): δ 7.54 (m, 6 H, C$_6$H$_5$), 7.45 (d, $^3J_{HH}$ = 6 Hz, 4 H, C$_6$H$_5$), 4.98 (s, 4 H, CH_2), 1.32 (m, 18 H, Bu^t), 1.26 (m, 36 H, Bu^t), −5.70 (dt with satellites, $^2J_{HP}$ = 8.6, $^3J_{HP}$ = 20.6, $^1J_{HPt}$ = 1367 Hz, 1 H, Pt−*H*) ppm. ^{13}C{^{1}H} NMR (CDCl$_3$, 293 K): δ 130.9 (s, Ph), 130.2 (s, Ph), 129.2 (s, Ph), 50.3 (s, *C*H$_2$Ph), 40.7 (s, P*C*Me), 40.3 (s, P*C*Me), 36.2 (s, PC*C*H$_3$), 35.4 (s, PC*C*H$_3$) ppm. IR (Nujol, KBr): 2140, 2119 (ν_{CN}) cm^{-1}.

Preparation of Pt$_3$(μ-PBu$^t_2$)$_3$(H)(CNC$_6$H$_4$-*p*-CH$_3$)$_2$ (6). A toluene (5.6 mL) solution containing 0.46 mmol of *p*-CH$_3$C$_6$H$_4$-NC was added to an orange solution of complex **1** (180 mg, 0.167 mmol) in toluene (5 mL). The solution quickly turned brown, and the solvent was evaporated; the residue was suspended in acetonitrile (6 mL) and left overnight at −30 °C. The brown solid was separated by filtration and vacuum-dried (190 mg, 82% yield).

Anal. Calcd for C$_{40}$H$_{69}$N$_2$P$_3$Pt$_3$: C, 38.2; H, 5.50; N, 2.23. Found: C, 38.6; H, 5.36; N, 2.15. ^{1}H NMR (CDCl$_3$, 293 K): δ 7.31 (d, 4 H, C$_6$H$_4$), 7.23 (d, 4 H, C$_6$H$_4$), 2.36 (s, 6 H, CH_3), 1.33 (d, $^3J_{HP}$ = 12 Hz, 18 H, Bu^t), 1.31 (d, $^3J_{HP}$ = 14 Hz, 36 H, Bu^t), −5.53 (dt with satellites, $^2J_{HP}$ = 9, $^3J_{HP}$ = 19, $^1J_{HPt}$ = 1360 Hz, 1 H, Pt−*H*) ppm. ^{13}C{^{1}H} NMR (CDCl$_3$, 293 K): δ 137.6 (s, *C*N), 130.2 (s, *C*$_6$H$_4$), 124.6 (s, *C*$_6$H$_4$), 38.6 (s, P*C*Me), 36.2 (s, P*C*Me), 34.2 (s, PC*C*H$_3$), 33.4 (s, PC*C*H$_3$), 21.5 (s, C$_6$H$_4$*C*H$_3$) ppm. IR (Nujol, KBr): 2104, 2044 (ν_{CN}) cm^{-1}.

Preparation of Pt$_3$(μ-PBu$^t_2$)$_3$(H)(CNBu^t)$_2$ (7). A toluene (4.33 mL) solution containing 0.38 mmol of Bu^{t}NC was added to an orange solution of complex **1** (180 mg, 0.167 mmol) in toluene (6 mL). The solution quickly turned violet, and the solvent was evaporated; the residue was suspended in *n*-hexane (6 mL) and left overnight at −30 °C. The violet solid was separated by filtration and vacuum-dried (147 mg, 70% yield).

Anal. Calcd for C$_{34}$H$_{73}$N$_2$P$_3$Pt$_3$: C, 34.3; H, 6.15; N, 2.35. Found: C, 34.4; H, 6.25; N, 2.35. ^{1}H NMR (CDCl$_3$, 253 K): δ 1.57 (s, 18 H, CNBu^t), 1.21 (m, 54 H, PBu^t), −4.30 (broad t with satellites, $^2J_{HP}$ = 8, $^1J_{HPt}$ = 1536 Hz, 1 H, Pt−*H*) ppm. ^{13}C{^{1}H} NMR (CDCl$_3$, 293 K): δ 34.1 (s, P*C*Me), 33.3 (s, PC*C*H$_3$), 30.1 (s, CNC*C*H$_3$) ppm. IR (Nujol, KBr): 2128, 2087 (ν_{CN}) cm^{-1}.

Preparation of Pt$_3$(μ-PBu$^t_2$)$_3$(Cl)(CNBu^t)$_2$ (8). A violet solution of complex **7** (40 mg, 0.033 mmol) in chloroform (4 mL) was stirred overnight at 60 °C. The solvent was evaporated, and the residue was suspended in *n*-hexane (5 mL). A violet solid was separated by filtration and vacuum-dried (25 mg, 62%).

Anal. Calcd for C$_{34}$H$_{72}$ClN$_2$P$_3$Pt$_3$: C, 33.4; H, 5.89; N, 2.29. Found: C, 32.9; H, 5.86; N, 2.29. ^{1}H NMR (CDCl$_3$, 253 K): δ 1.55 (s, 18 H, CNBu^t), 1.30 (m, 54 H, PBu^t) ppm. ^{13}C{^{1}H} NMR

Table 4. Crystal Data and Structure Refinement.

	4	**7·0.5C$_6$H$_{14}$**
empirical formula	C$_{28}$H$_{58}$F$_6$O$_2$P$_4$Pt$_3$	C$_{34}$H$_{73}$N$_2$P$_3$Pt$_3$·0.5C$_6$H$_{14}$
fw	1249.89	1231.21
temp, K	293(2)	293(2)
wavelength, Å	0.71073	0.71073
cryst syst, space group	orthorhombic, *Pnma* (No. 62)	triclinic, *P*$\bar{1}$ (No. 2)
unit cell dimens		
a, Å	25.765(5)	11.122(2)
b, Å	17.300(4)	15.408(3)
c, Å	8.912(2)	15.447(3)
α, deg		71.82(1)
β, deg		86.74(1)
γ, deg		69.48(1)
V, Å^3	3972.4(14)	2351.2(8)
Z	4	2
ρ_{calcd}, Mg/m^3	2.090	1.739
μ, mm^{-1}	10.751	9.029
no. of data/restraints/params	2705/0/187	6021/5/394
R(*F$_o$*) (*I* > 2σ(*I*))^a	0.0669	0.0322
R$_w$(*F$_o^2$*) (*I* > 2σ(*I*))^b	0.1496	0.0754

^{a} $R(F_o) = \Sigma||F_o| - |F_c||/\Sigma|F_o|$. ^{b} $R_w(F_o^2) = [\Sigma[w(F_o^2 - F_c^2)^2]/\Sigma[w(F_o^2)^2]]^{1/2}$; $w = 1/[\sigma^2 (F_o^2) + (AQ)^2 + BQ]$ where $Q = [\text{Max}(F_o^2, 0) + 2F_c^2]/3$.

(CDCl$_3$, 293 K): δ 51.6 (s, CN*C*Me$_3$ 38.1 (s, P*C*Me), 33.7 (s, PC*C*H$_3$), 30.3 (s, CNC*C*H$_3$) ppm. IR (Nujol, KBr): 2128, 2087 (ν_{CN}) cm^{-1}.

Preparation of [Pt$_3$(μ-PBu$^t_2$)$_3$(CNBu^t)$_3$]Cl (9). Bu^{t}NC (42 μL, 0.37 mmol) was added to a chloroform (8 mL) solution of complex **1** (100 mg, 0.092 mmol). After it stood at room temperature for 1 h, the solution was concentrated to 2 mL and Et$_2$O was added. The violet solid which precipitated out was filtered and vacuum-dried (71 mg, 59%).

Anal. Calcd for C$_{39}$H$_{81}$ClN$_3$P$_3$Pt$_3$: C, 35.8; H, 6.20; N, 3.22. Found: C, 35.6; H, 6.25; N, 3.40. ^{1}H NMR (acetone-*d$_6$*, 293 K): δ 1.63 (s, 27 H, CNC*C*H$_3$), 1.27 (vt, $^3J_{HP}$ + $^5J_{HP}$ = 7 Hz, 54 H, PCC*H$_3$*) ppm. ^{13}C{^{1}H} NMR (acetone-*d$_6$*, 293 K): δ 59.3 (s, CNC*C*H$_3$), 38.4 (s, P*C*), 33.1 (s, PC*C*H$_3$), 29.6 (s, CNC*C*H$_3$) ppm. IR (Nujol, KBr): 2161 (ν_{CN}) cm^{-1}.

Complex **9** was also prepared (80% yield) by reacting **8** with an excess of Bu^{t}NC.

X-ray Crystallography. Crystal Structure Determination of 4. A suitable crystal of **4** (0.26 × 0.12 × 0.02 mm) was mounted on a glass fiber for the data collection that was carried out, at room temperature, on a Bruker P4 diffractometer. The cell parameters, calculated from the setting angles of 30 reflections having 5.5° < θ < 12.9°, are listed in Table 4, together with other structural details. Data were measured using a ω/2θ scan mode; a redundant set of data was collected in order to check the diffraction symmetry and the reliability of the absorption correction procedure. Three standard reflections were measured every 97 measurements. A total of 3523 intensities (2.9° < θ < 25.0°) was collected. After data reduction, the equivalent intensities were merged to give 2705 independent data (R_{int}, $\Sigma|F_o^2 - F_o(\text{mean})^2|/\Sigma[F_o^2]$ = 0.067), which were corrected for Lorentz and polarization factors and empirically (ψ-scan method)[15] for absorption.[16]

The structure was solved by Patterson and Fourier methods and refined by full-matrix least squares on *F*^{2}. All non-hydrogen atoms were refined anisotropically. The hydrogen atoms were refined with isotropic thermal factors and allowed to ride on the connected carbon atoms.

(15) North, C. T.; Phillips, C.; Mathews, F. S. *Acta Crystallogr.* **1968**, *A24*, 351.

(16) XSCANS, X-ray Single-Crystal Analysis System, release 2.1; Siemens Analytical X-ray Instruments Inc., Madison, WI, 1994. ENRAF-Nonius SDP V version 5.0, 1989.

The marked anisotropy present in the thermal ellipsoids of some methyl groups and in the ethylene ligand suggests the presence of orientational disorder.

All calculations were carried out using the SHELXTL crystallographic program.[17]

Crystal Structure Determination of $7 \cdot 0.5 C_6 H_{14}$. An air-stable, prismatic, red crystal of $[Pt_3(\mu\text{-}PBu^t{}_2)_3(CN^tBu)_2(H)] \cdot 0.5 C_6 H_{14}$ ($7 \cdot 0.5 C_6 H_{14}$) was mounted on a Bruker SMART CCD diffractometer, equipped with a low-temperature device, for the unit cell determination and data collection. The cell constants were refined, at the end of the data collection, using 6040 reflections, with the data reduction software SAINT.[18] A total of 2142 frames were collected, by using an ω scan in steps of 0.3°, with a counting time of 20 s.

The intensities were corrected for Lorentz and polarization factors[18] and empirically for absorption using the SADABS program.[19] Selected crystallographic and other relevant data are listed in Table 4 and in Supplementary Table S6 (Supporting Information). The standard deviations on intensities were calculated in term of statistics alone, while those on $F_o{}^2$ were calculated as shown in Table 4. The structure was solved by direct and Fourier methods. The data were refined by full-matrix least squares,[20] minimizing the function $\sum w(F_o{}^2 - (1/k)F_c{}^2)^2$. During the refinement, anisotropic displacement parameters were used for all atoms, except the hydrogens, which were treated isotropically. Toward the end of the refinement, a disordered solvent molecule, lying across a symmetry center, was located in a difference Fourier map. Due to the orientational disorder, it was necessary to constrain the carbon–carbon separations at their expected values, using the slack constraints option in the SHELX program.[21] Moreover, a peak in an acceptable position for the hydride ligand was also found and refined without constraint, using an isotropic temperature factor. However, as expected, only a limited

precision in the position of the hydride ligand has been achieved (Pt–H = 1.51(7) Å). No extinction correction was deemed necessary. Upon convergence (see Supplementary Table S6 in the Supporting Information) the final difference Fourier map showed no significant peaks. The contribution of the hydrogen atoms, in their calculated positions (C–H = 0.95 Å, $B(\text{H}) = 1.5[B(\text{C}_{\text{bonded}})]$ Å^2), was included in the refinement using a riding model. All calculations were carried out by using the PC version of the SHELX-97 programs.[20] The scattering factors used, corrected for the real and imaginary parts of the anomalous dispersion, were taken from the literature.[21] The structure of $[Pt_3(\mu\text{-}PBu^t{}_2)_3(CN^tBu)_2(H)] \cdot 0.5\ C_6 H_{14}$ ($7 \cdot 0.5 C_6 H_{14}$) was also determined at room temperature by using a crystal obtained in a separate preparation and recrystallized from n-hexane (see the Supporting Information).

Further details about collection and refinement with full lists of atomic parameters for both the crystal structures described in this paper have been deposited in the form of CIF files with the Cambridge Crystallographic Database (Dep. No. CCDC 175513 and 175514 for compounds **4** and **7**, respectively).

Supporting Information Available: Text giving experimental details and full listings of crystallographic data for compounds **4** and **7**, including tables of positional and isotropic equivalent displacement parameters, calculated positions of the hydrogen atoms, anisotropic displacement parameters, and bond distances and angles and ORTEP diagrams showing the full numbering schemes. This material is available free of charge via the Internet at http://pubs.acs.org.

OM020027M

(17) Sheldrick, G. M. SHELXTL-Plus, Release 5.1; Bruker Analytical X-ray Instruments Inc., Madison, WI, 1997.

(18) SAINT: SAX Area Detector Integration; Siemens Analytical Instrumentation, Madison, WI, 1996.

(19) Sheldrick, G. M. SADABS; Universitat Göttingen, Göttingen, Germany, 1997.

(20) Sheldrick, G. M. SHELX-97: Structure Solution and Refinement Package; Universität Göttingen, Göttingen, Germany, 1997.

(21) *International Tables for X-ray Crystallography*; Wilson, A. J. C., Ed.; Kluwer Academic: Dordrecht, The Netherlands, 1992; Vol. C.